Competitive role of the tellurium and gadolinium cations in structural aspects of the gadolinium–phosphate–tellurate glasses

ARTICLE *in* JOURNAL OF ALLOYS AND COMPOUNDS · FEBRUARY 2010

Impact Factor: 3 · DOI: 10.1016/j.jallcom.2009.09.174

Journal of Alloys and Compounds 490 (2010) 270–276

Contents lists available at ScienceDirect

Journal of Alloys and Compounds

journal homepage: www.elsevier.com/locate/jallcom

Competitive role of the tellurium and gadolinium cations in structural aspects of the gadolinium–phosphate–tellurate glasses

S. Rada [a,*], M. Culea [b], M. Rada [a], T. Rusu [a], E. Culea [a]

[a] Technical University of Cluj-Napoca, 400641 Cluj-Napoca, Romania
[b] Faculty of Physics, Babes-Bolyai University of Cluj-Napoca, 400084 Cluj-Napoca, Romania

ARTICLE INFO

Article history:
Received 10 July 2009
Received in revised form
29 September 2009
Accepted 30 September 2009
Available online 6 October 2009

Keywords:
Glasses and glass ceramics
FT-IR spectroscopy
Semiempirical calculations

ABSTRACT

Glasses and glass ceramics in the ternary $xGd_2O_3(100-x)[7TeO_2{\cdot}3P_2O_5]$ systems with $0 \le x \le 70$ mol.% have been prepared from melt quenching method. Main results of the quantum–chemical calculation of the structural model for the $7TeO_2{\cdot}3P_2O_5$ glass network show that there is a charge transfer between the tellurium atoms coordinated +3 and +4 and between the tellurium atoms coordinated +4 with the phosphate network.

Presence of the multiple cations of gadolinium and tellurium in the glasses to attract the $[PO_4]$ structural units for compensation of charge yield a competition between these cations showing the drastic reduction of the characteristic features corresponding to the $[PO_4]$ structural units in bandwidth, position and intensity. After the heat treatment applied at 500 °C for 24 h, two crystalline phases appear, namely the $Te_4P_2O_{13}$ and $GdPO_4$. The $Te_4P_2O_{13}$ crystalline phase is characteristically of the host glass ceramic. The strong affinity of the Gd^{3+} ions towards the phosphorus groups containing non-bridging oxygen is responsible for the disappearance of $Te_4P_2O_{13}$ crystalline phase. The addition of higher Gd_2O_3 content yields the gradual depolymerization of the phosphate chains and the formation of the $GdPO_4$ crystalline phase.

1. Introduction

In the two past decades, tellurate glasses have attracted a great deal of interest [1–3], due to their potential use fiber amplifiers and non-linear optical devices [4,5]. Tellurate glasses are characterized by good chemical durability, low glass transition, high refractive index and high transmittance especially in near to middle infrared regions [6–9]. Tellurate glasses are also important for enhanced electrical properties [10–16]. Tellurium dioxide is a conditional glass former. It is very difficult to form pure vitreous TeO_2 [17].

Phosphate glasses are relatively easy to prepare and offer an important range of compositional possibilities, which facilitate tailoring of the physical and chemical properties of interest for specific technological applications [18–27].

For clarifying the structure of the binary tellurate glasses some works are done in analyzing the basic structural units whereby $[TeO_4]$ trigonal bypiramid and $[TeO_3]$ trigonal pyramids are found in crystals [28,29] and in glasses [30]. Despite some previous reports, the structure of binary tellurate glasses is still subject of discussion [31,32] because the addition of glass network modifier causes the network to break.

This paper will focus on immobilization of gadolinium oxide in tellurate–phosphate glasses and compare their structural properties. Thus, the aim of the present paper is to study the structure and the devitrification behavior of glasses in the TeO_2–P_2O_5 system, having the molar ratio of 7:3, by infrared spectroscopy and semiempirical calculations.

2. Experimental

The $xGd_2O_3(100-x)[7TeO_2{\cdot}3P_2O_5]$ glasses were prepared by mixing together desired amounts of TeO_2, H_3PO_4 and Gd_2O_3 in a ceramic crucibles. The crucible was transferred to a furnace for 20 min at 1100 °C. The glassy sample was subject to heat treatment applied at 500 °C for 24 h.

The samples were analyzed by means of X-ray diffraction using a XRD-6000 Shimadzu diffractometer, with a monochromator of graphite for the Cu Kα radiation (λ = 1.54 Å) at room temperature.

The structure of the glasses was investigated by infrared spectroscopy using the KBr pellet technique. The IR spectra were recorded in the range 400–1400 cm^{-1} using a JASCO FT-IR 6200 spectrophotometer.

The starting structures have been built using the graphical interface of Spartan'04 [33] and preoptimized by molecular mechanics. Dangling bonds of outer atoms of the models were saturated with hydrogen atoms. The structural geometry of the proposed phosphate–tellurate glass was completely optimized at PM3 levels (semiempirical method) [34]. The vibrational frequencies and the IR absorption intensities were calculated for the equilibrium geometry.

* Corresponding author.
E-mail addresses: Simona.Rada@phys.utcluj.ro, radasimona@yahoo.com (S. Rada).

0925-8388/$ – see front matter © 2009 Elsevier B.V. All rights reserved.
doi:10.1016/j.jallcom.2009.09.174

3. Results and discussion

3.1. Structural studies on untreated and heat-treated $7TeO_2{\cdot}3P_2O_5$ samples

The X-ray diffraction patterns for untreated and heat-treated $7TeO_2{\cdot}3P_2O_5$ samples are shown in Fig. 1. The figure did not reveal any crystalline phase in the glass sample. After heat treatment, the $Te_4P_2\ O_{13}$ crystalline phase was detected in the sample.

The examination of the FT-IR spectra of the $7TeO_2{\cdot}3P_2O_5$ glass and glass ceramic (Fig. 2) shows that the heat treatment modifies the characteristic IR bands as follows:

(i) The feature of band centered at about ~503 cm^{-1} splits into two new bands located at 450 and 501 cm^{-1}. These bands are attributed to the deformation modes of the P–O bonds from the $[PO_4]$ structural units [35].
(ii) The band constituted from two characteristic features at 625 and 730 cm^{-1} slips into three components located at ~610, 650, 680 cm^{-1}. These bands were assigned to the Te–O bending and stretching vibrations in $[TeO_4]$ units [36,37]. New shoulders appear at about 730 cm^{-1} and 820 cm^{-1}. These shoulders can be due to the presence of diphosphate units which are typical of the P_2O_7 groups [38] and the $[TeO_3]$ structural units [39].

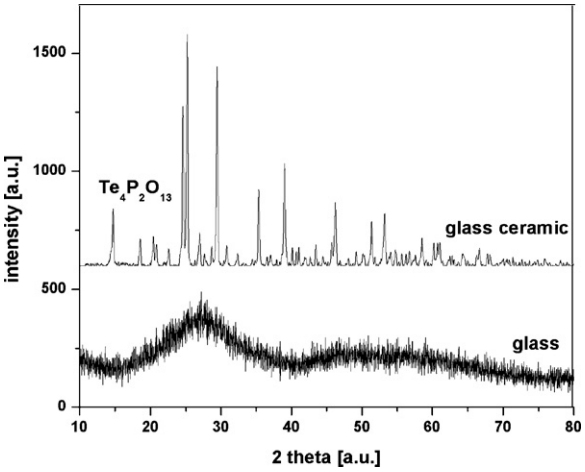

Fig. 1. X-ray diffraction patterns for untreated and heat-treated $7TeO_2{\cdot}3P_2O_5$ samples.

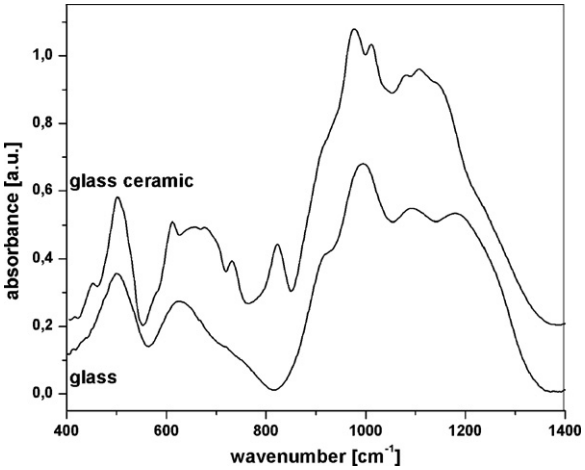

Fig. 2. FT-IR spectra of the $7TeO_2{\cdot}3P_2O_5$ glass and glass ceramic.

(iii) The feature of the band centered in the region ~994 cm^{-1} splits into two new bands located at 975 and 1014 cm^{-1}. These bands were associated to the vibrations in the orthophosphate structural units.
(iv) The feature of band from ~1100 cm^{-1} splits into two new bands located at 1078 and 1108 cm^{-1}. These bands can be due to the vibrations of PO_2 of the metaphosphate units [40].
(v) The band centered at ~1187 cm^{-1} is assigned to the PO_2 symmetric stretching mode and the P–O–P stretch of $[PO_4]$ tetrahedral sharing corners [41].

Taking into account these changes of the IR spectral features induced by the heat treatment, we can conclude that in the heat-treated samples there are more types of ortophosphate and diphosphate structural units. These structural units yield the depolymerization of the phosphate glass network and the apparition of the $Te_4P_2O_{13}$ crystalline phase.

In brief, the significantly different shape of the IR spectrum for treated samples compared to that untreated samples reveals a drastic structural change occurring between these compositions due to the apparition of the $Te_4P_2\ O_{13}$ crystalline phase, in agreement to the X-ray data.

3.2. Semiempirical calculations

In general, we notice a good agreement between the experimental and calculated values of the lengths of the Te–O and of P–O bonds in the characteristic structural units (1.9–2.1 Å for the length of Te–O bond and 1.66–1.73 Å for the length of P–O bond). The calculated Te–O and P–O bond lengths in the $[TeO_4]$, $[TeO_3]$ and $[PO_4]$ groups agree well with the experimental data available in the literature (in particular obtained using neutron diffraction) [42–44].

For some $[PO_4]$ groups the lengths of P–O bonds are somewhat longer than the P–O covalent bond but significantly shorter than the sum of the van der Waals radii suggesting an asymmetrical coordination in the $[PO_4]$ tetrahedral structural units (Fig. 3). Instead we meet to regular coordination polyhedron of tellurium ions which explain probably an increase of the strength of P–O–Te bonds and the improved of the chemical durability.

The quantum–chemical calculations of IR absorption spectra reveal that the proposed model for phospho-tellurate is in good agreement with the experimental IR absorption spectra (Fig. 4).

The band gap of our model can be estimated as the eigenvalue difference between a highest occupied molecular orbital (homo) and a lowest unoccupied molecular orbital (lumo) [45]. The homo–lumo gap is 4.2 eV. The distribution of the electronic states of the homo, homo(−1) and lumo, lumo(−1) can be seen in Fig. 5. An interesting finding in this system is that:

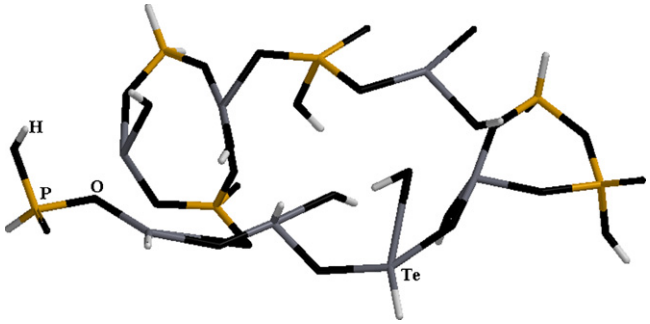

Fig. 3. Optimized structure of the model for binary $7TeO_2{\cdot}3P_2O_5$ glass.

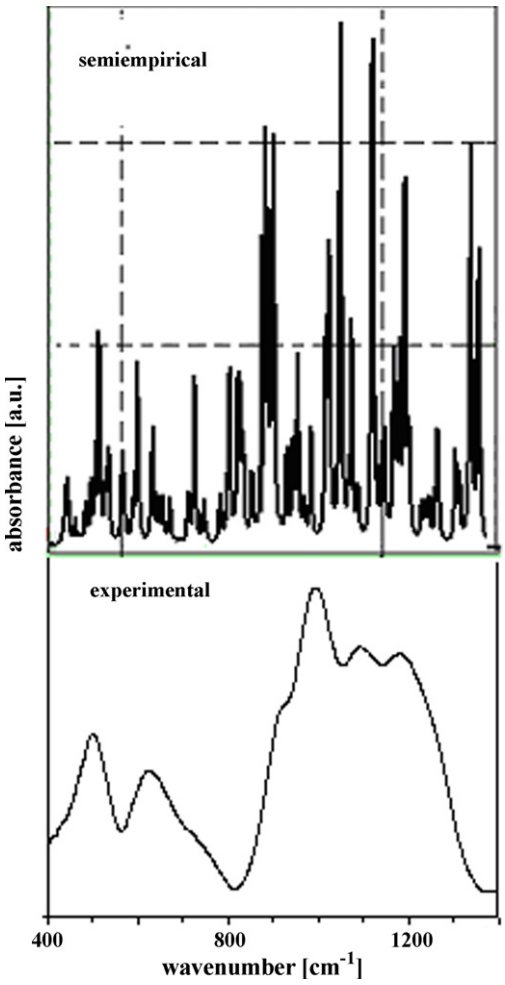

Fig. 4. Simulated IR spectrum using semiempirical calculations of the proposed model for $7TeO_2{\cdot}3P_2O_5$ glassy.

(i) The homo and homo(−1) give the character of electron donor for the [TeO_4] units of the tellurate network.
(ii) The lumo and lumo(−1) give the character of acceptor electron for the [TeO_3] of the tellurate units and the [PO_4] units of phosphate network.

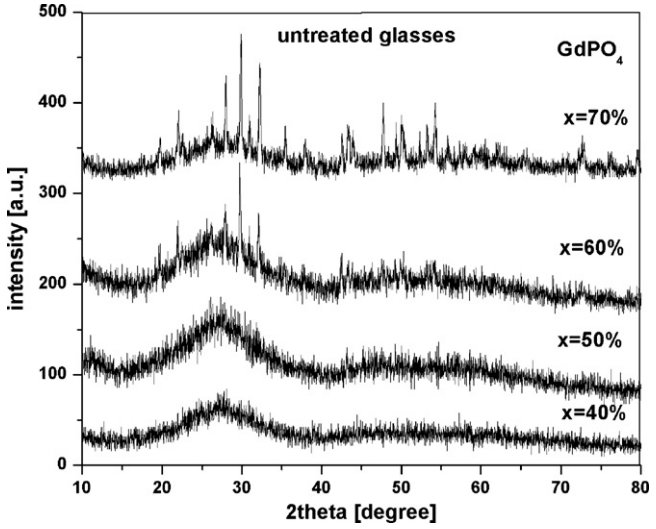

Fig. 6. X-ray diffraction patterns for $xGd_2O_3(100-x)[7TeO_2{\cdot}3P_2O_5]$ samples.

There is a change transfer between the tellurium atoms coordinated +3 and +4 and the tellurium atom coordinated +4 with the phosphate network.

In brief, the heat treatment leads depolymerization of the phosphate network by the increase of orthophosphate structural units. The stabilization of the phosphate structural units can be achieved by several metallic cations, namely tellurium ions.

3.3. Structural properties of the $xGd_2O_3(100-x)[7TeO_2{\cdot}3P_2O_5]$ glasses

The X-ray diffraction patterns did not reveal any crystalline phase in the prepared samples up to 50 mol.% Gd_2O_3. By increasing the concentration of gadolinium ions up to 60 mol.% Gd_2O_3, the $GdPO_4$ crystalline phase was detected in the samples (Fig. 6).

It is known that pure tellurate structures consist of four main bands: two stronger bands at 680 and 780 cm^{-1} are due to the Te–O stretching vibrations of the [TeO_4] and [TeO_3] structural units, and two weaker bands at 520 and 930 cm^{-1} belong to the vibrations of Te–O–Te bridging bonds and $Te–O^-$ non-bridging bonds in [TeO_3] structural units [39].

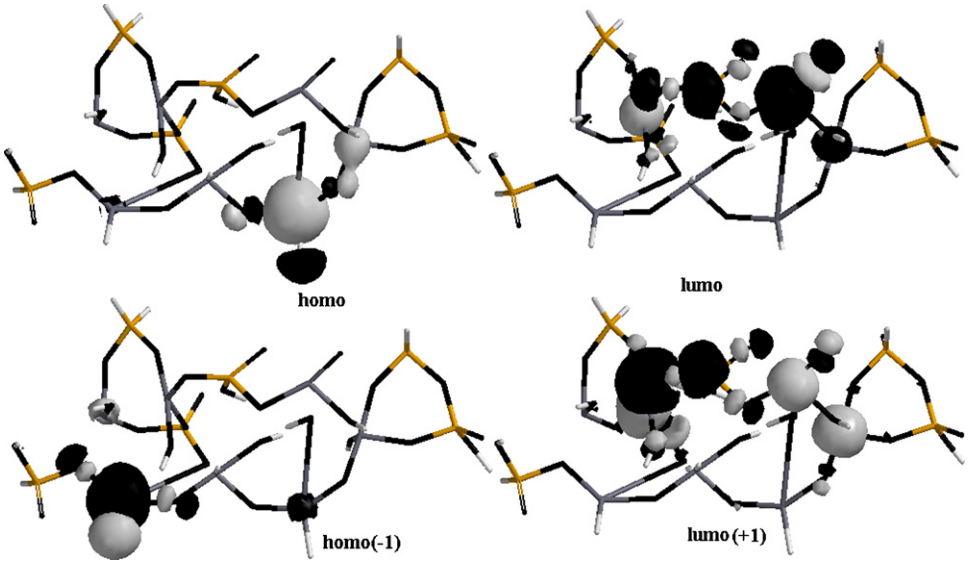

Fig. 5. The distribution of the electronic states of the homo, homo(−1) and lumo, lumo(−1) of the proposed model for $7TeO_2{\cdot}3P_2O_5$ glassy.

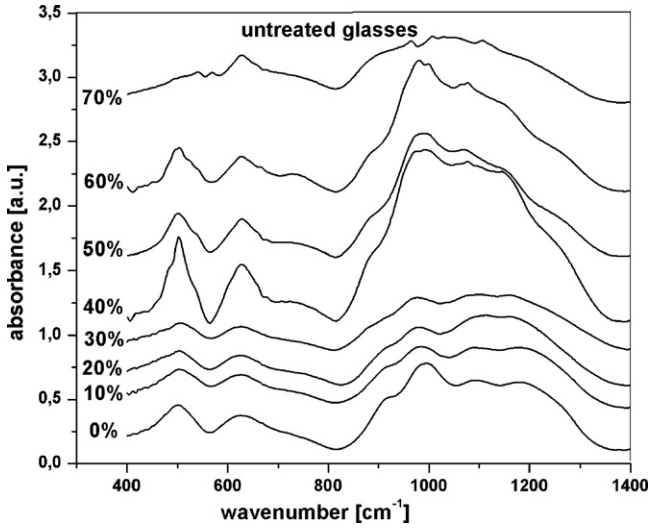

Fig. 7. FT-IR spectra of the $x Gd_2O_3(100-x)[7TeO_2{\cdot}3P_2O_5]$ samples.

P_2O_5 is a well-known strong glass forming oxide, participates in the glass network with $[PO_4]$ structural units. One of the four oxygen atoms in $[PO_4]$ tetrahedron is doubly bonded to the phosphorus atom with the substantial π-bond character to account for pentavalence of phosphorous. The $[PO_4]$ tetrahedrons are linked together with covalent bonding in chains are linked together by crossbonding between the metal cation and two non-bridging oxygen atoms of each $[PO_4]$ tetrahedron.

The experimental FT-IR spectra of $xGd_2O_3(100-x)[7TeO_2{\cdot}3P_2O_5]$ system with various contents of gadolinium oxide ($0 \le x \le 70$ mol.%) consisting of broad peaks and shoulders are presented in Fig. 7. Obtained bands and their assignments can be summarized as follows:

(i) The band located at about 530 cm^{-1} is attributed to the deformation modes of the P–O bonds from the $[PO_4]$ structural units.
(ii) The larger band centered at ~625 cm^{-1} is assigned to the stretching mode of the $[TeO_4]$ trigonal bypiramidal with bridging oxygens [41]. The shoulder located at about 750 cm^{-1} indicates the presence of $[TeO_3]$ structural units.
(iii) The feature of band centered in the region ~994 cm^{-1} can be due to the vibrations in orthophosphate structural units. The position of band from ~1100 cm^{-1} corresponds to the vibrations of PO_2 of metaphosphate groups. The band centered at ~1175 cm^{-1} is assigned to the PO_2 symmetric stretching mode and the P–O–P stretch of $[PO_4]$ tetrahedral sharing corners. The shoulder near ~900 cm^{-1} is assigned to the asymmetric stretching mode.
(iv) A new shoulder appears at about 873 cm^{-1} which correspond to the P–O vibrations in pyrophosphate structural units.
(v) The intensity of the band from ~995 cm^{-1} decreases with the increase of Gd_2O_3 content and shifts to ~975 cm^{-1}. This band is due to the P–O stretching vibrations in orthophosphate units.
(vi) By increasing of Gd_2O_3 content up to 70 mol.%, the intensities of the bands centered at about 1100 and 1195 cm^{-1} increase. The position of these bands is found to be shifted towards lower wave number with Gd_2O_3 concentration (~1094 and 1161 cm^{-1}, respectively).

The general trend in the intensity of the IR spectra is to increase with Gd_2O_3 content in the region between 400 and 1400 cm^{-1}, except to the intensity in the region 400–800 cm^{-1} which it is remained almost unaffected for sample with $x \le 30$ mol.%. This suggests that the glass network modification has taken place mainly in the phosphate part whereas the tellurate part remained unmodified for the $[TeO_3]$ structural units. Thus, the gadolinium phosphate–tellurate glasses network exists mostly as the $[TeO_4]$, $[PO_4]$ tetrahedral units, and some $[TeO_3]$ structural units and with interconnected through P–O–P bridges in $[PO_4]$ structural units.

Based on these experimental results, we propose that the compositional evolutions of the structures of the glass can be explained considering two different mechanisms:

(i) By increasing of Gd_2O_3 content up to 20 mol.%, the orthophosphate structural units convert to the phosphate and pyrophosphate structural units up to the maximum. In this manner the excess oxygen added to the glass upon addition of the Gd_2O_3, is taken up by transforming of orthophosphate units to meta- and pyrophosphate units and the excess negative charge is compensated by nearby gadolinium ions. In addition, non-bridging oxygen's do not frame. The conversion of orthophosphate units does not continue further because begins the formation of the isolated orthophosphate units and the conversion orthophosphate back to meta- and pyrophosphate units concomitant with the formation of the non-bridging oxygen's.
(ii) With increasing Gd_2O_3 content up to 20 mol.%, the compositional evolution was followed by a conversion of orthophosphate back to meta- and pyrophosphate. The excess of Gd_2O_3 causes formation of pyrophosphate rings of $[PO_4]$ tetrahedral structural units (the band located at about 875 cm^{-1}) in the general, vicinity of the gadolinium captions. Beyond this point, network continuity breaks down with the formation of larger numbers of non-bridging oxygen's yielding the apparition of the $GdPO_4$ crystalline phase, in agreement with the X-ray diffraction.

Presence of multiple cations of gadolinium and tellurium in the glasses to attract the $[PO_4]$ structural units for compensation of charge yield a competition between these captions. This preference is decided by the potential of ionization of the cations. This competition explains the drastic reduction of the characteristic features corresponding to the $[PO_4]$ structural units in bandwidth, position and intensity. In order to understand the theoretical data of the IR spectrum concerning to the vibrations of the massive $[PO_4]$ units, the samples were subject to heat treatment.

3.4. Structural properties of the heat-treated $xGd_2O_3(100-x)[7TeO_2{\cdot}3P_2O_5]$ samples

The vitreous or/and crystalline nature of the $xGd_2O_3{\cdot}(100-x)[7TeO_2{\cdot}3P_2O_5]$ glass system with various contents of gadolinium oxide ($0 \le x \le 50$ mol.%) was tested by X-ray diffraction. After heat treatment applied at 500 °C for 24 h, some structural changes were observed and two crystalline phases appeared in the structure of the samples, namely the $Te_4P_2O_{13}$ (for samples with $0 \le x \le 20$ mol.%) and $GdPO_4$ ($x > 50$ mol.%) (Fig. 8). Two halos characteristic of the amorphous compounds can be observed in these figures for samples with $10 \le x \le 50\%$ Gd_2O_3.

The FT-IR spectra of glass ceramics samples are reported in Fig. 9. The heat-treated samples matrix shows some changes in the FT-IR spectra with the increasing of the Gd_2O_3 content. The IR bands of the heat-treated samples and their assignments can be summarized as follows:

(i) By increasing of Gd_2O_3 content up to 30%, the characteristic feature of the shoulder located at about 425 cm^{-1} disappears, after that its appears at 40% Gd_2O_3 composition. This band is assigned the bending mode of Te–O–Te or O–Te–O linkages. The intensity of the band centered at about 500 cm^{-1} increases

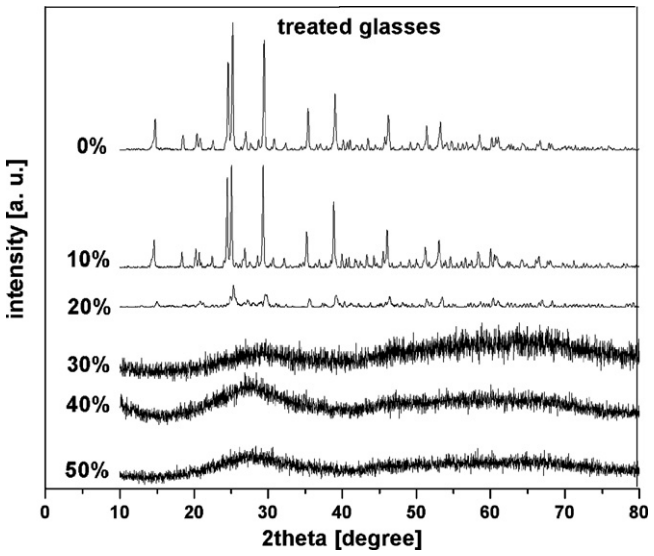

Fig. 8. X-ray diffraction patterns for heat-treated $x Gd_2O_3(100-x)[7TeO_2{\cdot}3P_2O_5]$ samples with $x = 0$–50% Gd_2O_3.

and shifts to ~520 cm^{-1}. A new band corresponding to the bending modes of the $[PO_4]$ groups appears at about 520 cm^{-1}.

(ii) The prominent band centered at about 635 cm^{-1} splits into three new components located at ~609, 656 and 698 cm^{-1} assigned to the bending and stretching Te–O vibrations in $[TeO_4]$ units. Its feature is more modified and shifts to ~630 cm^{-1} with increasing of Gd_2O_3 content.

(iii) The shoulder located at about 730 cm^{-1} is due to the presence of diphosphate units which are typical of the P_2O_7 groups [36]. Its intensity increases with the increase of Gd_2O_3 content. The band consisting of two characteristic features located at ~975 and 1000 cm^{-1} were shifted to 978 cm^{-1} by increasing of the Gd_2O_3 content up to 50%. The position of the bands from ~1100 and 1150 cm^{-1} is found to be shifted toward smaller wave number (1074 and 1138 cm^{-1}) with the increasing of Gd_2O_3 content.

In order to see the quantitative estimation of the distribution of the various species represented by FT-IR spectra, we will calculate the distribution by structural units based on the acid–base concept. Moreover, presence of multiple oxides in the glass always increases the tendency of the network formers to attract oxygen ions due to competition between the cations themselves. This preference is decided by the electronegativity of the structural groups [46,47]. The unit which has higher electronegativity value picks up oxygen ion and gets modifier. This tendency increases further if the size of cations increases. A possible mechanism which explains the scheme of the structural modifications it is represented on the basis of following equations:

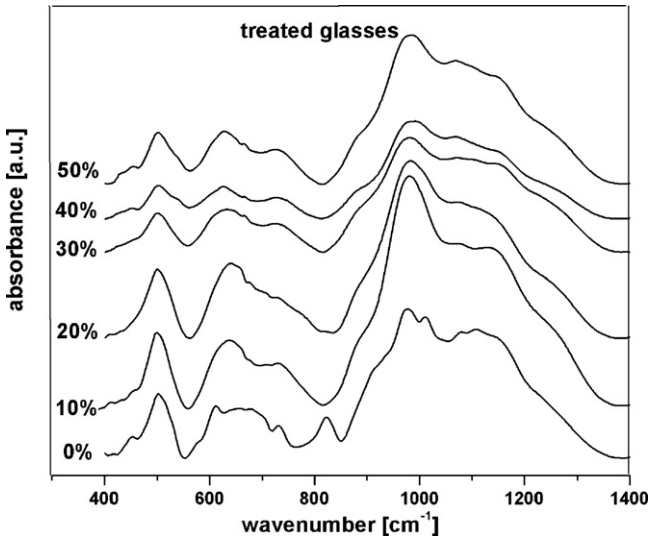

Fig. 9. FT-IR spectra of the heat-treated $x Gd_2O_3(100-x)[7TeO_2{\cdot}3P_2O_5]$ samples with $x = 0$–50% Gd_2O_3.

(i) The species present in the sample with $x = 0$ are $Te_4P_2O_{13}$ crystalline phase, and Te_3O_8, $2[P_2O_{7/2}]$ structural units. The modifier and former roles of the P_2O_5, TeO_2 and Gd_2O_3 can be represented as:

$$Gd_2O_3 \rightarrow 2Gd^{3+} + 3O^{2-}$$

$$P_2O_5 \equiv 2[PO_{3/2}]$$

$$2TeO_2 \equiv 2[TeOO_{2/2}]^0$$

(ii) For Gd_2O_3 content up to 20 mol.%, the gadolinium ions are firstly inserted in the trivalent state and they can be considered as modifiers because they have a strong affinity towards these groups containing non-bridging oxygens, which are negative-charged. Presence of multiple cations, phosphorus and tellurium in the glass ceramic to attract oxygen ions yield a competition between these cations. The P_2O_5 (2.19) has higher electronegativity than TeO_2 (2.10) [39]. The following reactions should occur in this region:

$$Te_3O_8 + O^{2-} \rightarrow [TeO_{4/2}] + Te_2O_6$$

$$2[P_2O_{7/2}] + 2Gd^{3+} + 2O^{2-} \rightarrow 2[O{=}P{-}O_{3/2}]Gd + 2[PO_{4/2}]^0$$

It was found that the intensity of the absorption band located in the region of 900–1000 cm^{-1} attains its maximum value at 10 mol.% Gd_2O_3. This band can be due to the $[PO_4]$ orthophosphate unit's vibrations.

(iii) For $x > 20$ mol.% Gd_2O_3, gadolinium ions will participate in the network as modifiers for $[PO_4]$ structural units from $Te_4P_2O_{13}$ crystalline phase yielding its disappearance. This may be attributed to the electrostatic field of the strongly polarizing Gd^{3+} ions. The increase of Gd^{3+} content leads to strengthening the electron cloud around oxygen in $[PO_4]$ units, and consequently causes a shift of the bands corresponding to the $[PO_4]$ structural units to lower wave number. This effect yields the connection of oxygen ions between diverse $[PO_4]$ polyhedrons (the new band appears at about 730 cm^{-1}).

$$2[O{=}P{-}O_{3/2}]Gd + O^{2-} \rightarrow 2[PO_2O_{2/2}] + 2Gd^{3+}$$

$$2Gd^{3+} + Te_4P_2O_{13} \rightarrow 4[TeOO_{2/2}] + 2[O{=}P{-}O_{3/2}]Gd$$

$$2[O{=}P{-}O_{3/2}]Gd + 4[TeOO_{2/2}] \rightarrow 4[TeO_{3/2}] + 2[O{=}P{-}O_{3/2}] + Gd^{3+} + 2O^{2-}$$

$$Gd^{3+} + 2[TeO_{4/2}] \rightarrow 2[TeO_{3/2}] + Gd^{3+} + O^{2-}$$

$$2[O{=}P{-}O_{3/2}] + 2[PO_2O_{2/2}] + 2[PO_{4/2}]^0 \rightarrow P_6O_{15}$$

$$Te_2O_6 + 2O^{2-} \rightarrow 2[TeO_4]$$

$$2[TeO_{3/2}] + O^{2-} \rightarrow 2[TeO_{4/2}]$$

The detailed study on IR spectra of $xGd_2O_3(100-x)[7TeO_2{\cdot}3P_2O_5]$ glass ceramics show that Gd_2O_3 content causes some drastic structural modifications (the gradual disappearance of $Te_4P_2O_{13}$ crystalline phase) which lead to the decrease in the connectivity and the decrease in the glass transition temperature.

Structural changes, as recognized by analyzing band shapes of IR spectra, revealed that the Gd_2O_3 high content causes a change from the phosphate network to the tellurate–phosphate network with interconnected through Te–O–P, P–O–P and Te–O–Te bridges. This competition between cations of gadoliunium and tellurium to attract the $[PO_4]$ structural units for compensation of charge explains the drastic reduction of the characteristic features corresponding to the $[PO_4]$ structural units in bandwidth, position and intensity.

The changes of the IR spectral features produced by the heat treatment suggest that the samples with x between 30 and 50 mol.% Gd_2O_3 show an increase of the degree of polymerization of the glass network. When, a high content of Gd_2O_3 (>20 mol.%) is introduced, more $[PO_4]$ structural units are coupled with gadolinium ions and the Te–O–Te linkages are deformed yielding the intercalation of $[TeO_n]$ entities in the $[PO_4]$ chain network. This in turn has led to a decrease in the connectivity yielding the formation of $GdPO_4$ crystalline phase which has been confirmed by XRD investigations ($x \geq 60$ mol.%).

For heat-treated samples, the decreasing trends of the bands located in the region 600–1300 cm^{-1} can be due to the formation of bridging bond of Te–O–P. Since the stretching force constant of Te–O bonding is substantially lower than that of the P–O, the stretching frequency of Te–O–P might trend to be lower. Such a behavior, namely the increase of the polymerization degree of the structural units with increasing the rare earth ion content by heat treatment was previously reported based on IR spectroscopy data for other glasses [38–51].

In brief, it is found that the vibration intensity of Te–O bond decreases as the Gd_2O_3 content increases. This fact indicates that the Gd^{3+} ions enter the phosphorus environment. The vibration bands of the $[PO_4]$ structural units appear until $x = 50$ mol.%. This fact reflects that when Gd^{3+} ions are added, more ions enter the phosphorus units coupling with P–O bonds of the $[PO_4]$ structural units. There are still a lot of Gd^{3+} ions existing in the tellurate units. They can be attributed to the influence of the lone pair electrons of tellurate units [47]. This strong affinity of the Gd^{3+} ions towards the phosphorus groups containing non-bridging oxygen [38,21,52] is responsible for the disappearance of $Te_4P_2O_{13}$ crystalline phase and the formation of the $GdPO_4$ crystalline phase.

The changes of the IR spectral features produced by devitrification suggest that the competition between cations of gadolinium and tellurium explains the drastic reduction of the characteristic features corresponding to the $[PO_4]$ structural units in bandwidth, position and intensity.

4. Conclusions

Transparent glass was easily obtained by cooling of the melts in air for studied composition. The devitrification behavior of the $7TeO_2{\cdot}3P_2O_5$ glasses examined by infrared spectroscopy and quantum mechanical calculations are reported.

The IR data show that the tellurium ions play the glass former role and increase the stability of the heat-treated glasses while the gadolinium ions contribute to the depolymerization of the heat-treated glass network. However, an inspection of the spectral features of the heat-treated glasses shows that these glasses contain the diphosphate structural groups together with the metaphosphate and orthophosphate structural units.

The gradual increase of gadolinium oxide in the glass over 20 mol.% results to transformation of some orthophosphate units to metaphophate and pyrophosphate units, disappearance of the P=O stretching bond in $[PO_4]$ tetrahedron. This in turn has led to a decrease in the connectivity and the formation of $GdPO_4$ crystalline phase.

After the heat treatment applied at 500 °C for 24 h, two crystalline phases appear, namely the $Te_4P_2O_{13}$ and $GdPO_4$. The $Te_4P_2O_{13}$ crystalline phase is characteristic of the host glass ceramic. The strong affinity of the Gd^{3+} ions towards the phosphorus groups containing non-bridging oxygen is responsible for the disappearance of $Te_4P_2O_{13}$ crystalline phase.

References

[1] E.M. Vogel, M.J. Weber, D.M. Krol, Phys. Chem. Glasses 32 (1991) 231.
[2] H.G. Kim, T. Komatsu, K. Shiota, K. Matusita, K. Tanaka, K. Hirao, J. Non-Cryst. Solids 208 (1996) 303.
[3] S.H. Kim, T. Yoko, J. Am. Ceram. Soc. 78 (1995) 1061.
[4] V. Dimitrov, S. Sakka, J. Appl. Phys. 79 (1996) 1741.
[5] J.J. Lin, W. Huang, Z. Sun, C.S. Ray, D.E. Day, J. Non-Cryst. Solids 336 (2004) 189.
[6] H. Burger, K. Kniepp, H. Hobert, J. Non-Cryst. Solids 15 (1992) 134.
[7] L.M.S. El-Deen, M.S.Al. Salhi, M.M. Elkholy, J. Alloys Compd. 465 (2008) 333.
[8] H.X. Yang, H. Lin, L. Lin, Y.Y. Zhang, B. Zhai, E.Y.B. Pun, J. Alloys Compd. 453 (2008) 493.
[9] C. Zhao, G.F. Yang, Q.Y. Zhang, Z.H. Jiang, J. Alloys Compd. 461 (2008) 617.
[10] A. Ghosh, J. Chem. Phys. 102 (1995) 1385.
[11] A. Ghosh, J. Phys.: Condens. Matter 1 (1989) 7819.
[12] A. Ghosh, Philos. Mag. 61 (1990) 87.
[13] A. Ghosh, A. Pan, Phys. Rev. Lett. 84 (2000) 2188.
[14] A. Pan, A. Ghosh, Phys. Rev. B 59 (1999) 899.
[15] A. Pan, A. Ghosh, Phys. Rev. B 60 (1999) 3224.
[16] D. Dutta, A. Ghosh, Phys. Rev. B 72 (2005) 024201.
[17] J.R. Van Wazer, Phosphorus and its Compounds, Interscience Publishers Ltd., London, 1958.
[18] A. Masingu, G. Piccaluga, G. Pnna, J. Non-Cryst. Solids 52 (1990) 29.
[19] S. Rani, S. Sanghi, A. Agarwal, N. Ahlawat, J. Alloys Compd. 477 (2009) 504.
[20] Y. Fang, L. Hu, M. Liao, L. Wen, J. Alloys Compd. 457 (2008) 19.
[21] N.K. Mohan, M.R. Reddy, C.K. Jayasankar, N. Veeraiah, J. Alloys Compd. 458 (2008) 66.
[22] M. Seshadri, K.V. Rao, J.L. Rao, Y.C. Ratnakaram, J. Alloys Compd. 476 (2009) 263.
[23] S.W. Martin, C.A. Angell, J. Am. Ceram. Soc. C-148 (1984) 67.
[24] W. Lutze, R.C. Erwing, Radioactive Waste Forms for the Future, Elsevier, Amsterdam, 1988.
[25] S.E. Haggerty, Ann. Rev. Earth Planet. Sci. 11 (1983) 133.
[26] G.D. Khattak, E.E. Khawaja, L.E. Wenger, D.J. Thompson, M.A. Salid, A.B. Hallak, M.A. Daous, J. Non-Cryst. Solids 194 (1996) 1.
[27] C.M. Jantzen, J. Non-Cryst. Solids 84 (1986) 215.
[28] J. Galy, O. Lindquist, J. Solid State Chem. 27 (1979) 279.
[29] Y. Dimitriev, V. Dimitriev, Mater. Res. Bull. 13 (1978) 1071.
[30] U. Hoppe, E. Yousef, C. Russesl, J. Neuefeind, A.C. Hannon, Solid State Commun. 123 (2002) 273.
[31] T. Sekiya, N. Mochida, S. Ogawa, J. Non-Cryst. Solids 176 (1994) 105.
[32] S. Rada, M. Culea, E. Culea, J. Non-Cryst. Solids 354 (52–54) (2008) 5491.
[33] Spartan'04, Wavefunction Inc., 18401 Von Karman Avenue, Suite 370 Irvine, CA 92612.
[34] M.J.S. Dewar, E.G. Zoebisch, E.F. Healy, J.J.P. Stewart, J. Am. Chem. Soc. 107 (1985) 3902.
[35] S. Rada, M. Culea, M. Rada, E. Culea, J. Mater. Sci. 43 (18) (2008) 6122.
[36] S. Rada, E. Culea, M. Culea, J. Mater. Sci. 43 (19) (2008) 6480.
[37] S. Rada, E. Culea, V. Rus, M. Pica, M. Culea, J. Mater. Sci. 43 (10) (2008) 3713.
[38] G.W. Anderson, W.D. Compton, J. Chem. Phys. 52 (1970) 6166.
[39] S. Rada, M. Culea, E. Culea, J. Phys. Chem. A 112 (44) (2008) 11251.

[40] J.O. Byun, B.H. Kim, S.K. Hong, H.J. Jung, S.W. Lee, A.A. Izyneev, J. Non-Cryst. Solids 190 (1995) 88.
[41] R.F. Bartholomew, J. Non-Cryst. Solids 7 (1972) 221.
[42] R. Iordanova, V. Dimitrov, Y. Dimitriev, J. Non-Cryst. Solids 180 (1994) 58.
[43] M. Abo-Naf, F.H.El. Batal, M.A. Azooz, Mater. Chem. Phys. 77 (2002) 846.
[44] A. Kumar, S.B. Rai, D.K. Rai, Mater. Res. Bull. 38 (2003) 333.
[45] T. Uchino, M. Iwasaki, T. Sakka, Y. Ogata, J. Phys. Chem. 95 (1991) 5455.
[46] V.O. Sokolov, V.G. Plotnichenko, V.V. Koltashev, E.M. Dianov, J. Non-Cryst. Solids 352 (2006) 5618.
[47] A. Chahine, M. Et-tabirou, M. Elbenaissi, M. Haddad, J.L. Pascal, Mater. Chem. Phys. 84 (2004) 341.
[48] S. Rada, E. Culea, J. Mol. Struct. 929 (2009) 141.
[49] S. Rada, E. Culea, M. Rada, P. Pascuta, V. Maties, J. Mater. Sci. 44 (2009) 3235.
[50] S. Rada, P. Pascuta, M. Culea, V. Maties, M. Rada, M. Barlea, E. Culea, J. Mol. Struct. 924–926 (2009) 89.
[51] S. Rada, M. Bosca, E. Culea, M. Rada, V. Dan, V. Maties, Struct. Chem. 20 (2009) 801.
[52] R.V.S.S.N. Ravikumar, A.V. Chandrasekhar, L. Ramamoorthy, B.J. Reddy, Y.P. Reddy, J. Yamauchi, P.S. Rao, J. Alloys Compd. 364 (2004) 176.